RSC Advances

This article can be cited before page numbers have been issued, to do this please use: L. Wang, S. Cao, Z. Du, Q. Wu, Z. Bian, C. Kang, L. Gao and J. Zhang, *RSC Adv.*, 2016, DOI: 10.1039/C6RA16686E.

ROYAL SOCIETY OF CHEMISTRY

www.rsc.org/advances

View Article Online
DOI: 10.1039/C6RA16686E

Journal Name

ARTICLE

4-Dimethylaminopyridine-catalyzed Dynamic Kinetic Resolution in Asymmetric Synthesis of *P*-Chirogenic 1,3,2-Oxazaphospholidine-2-Oxides

Received 00th January 20xx,
Accepted 00th January 20xx

DOI: 10.1039/x0xx00000x

www.rsc.org/

Lanlan Wang,[a, b] Shanshan Cao,[c] Zhijun Du,[a] Qiang Wu,[a, b] Zheng Bian,[a] Chuanqing Kang,*[a] Lianxun Gao[a] and Jingping Zhang[c]

Excellent diastereoselectivity (*dr* value up to 100:0) was achieved in DMAP-catalyzed P-N bond formation in the synthesis of *P*-chirogenic organophosphines from phenylphosphonic dichloride ($PhP(O)Cl_2$) and (*S*)-2-pyrrolidinemethanol derivatives. Investigations with NMR spectra and calculations revealed the formation of a bimolecular complex from ($PhP(O)Cl_2$) and revealed DMAP as an 'active phosphonyl' that was converted to the P-N bonded compound with significant preference for one of two diastereomers through dynamic kinetic resolution. These results present for the first time the mechanism of conversion from an achiral phosphorus centre to a *P*-stereogenic centre by direct stereoselective reaction at the phosphorus centre.

Introduction

Optically pure *P*-chirogenic organophosphorus compounds have become an active research interest with steady growth in the past two decades.[1] The distinctive geometry around the *P*-stereogenic centre, unlike *C*-centre, provides a criterion for chiral information transfer in organic conversion, polymeric conformation and supramolecular assemblies.[2] Successful applications of *P*-chiral organophosphines as organocatalysts or as ligands for metallocatalysis have spurred intensive research on these compounds, in particular, on the synthesis of *P*-chirogenic catalytic scaffolds.[3] Strategies for this synthesis include chiral skeletal modification, catalytic asymmetric synthesis, and thermodynamic or kinetic resolution. Limited chiral pools including ephedrine, menthanol and prolinols have been used for inducing diastereoselective reaction at the *P*-centre.[4] In those reactions, separation is usually unavoidable for accessing optically pure products. Ephedrine was most effective for inducing high stereoselectivity, however it is not commercially available due to possible abuse as a drug. Catalytic enantioselective synthesis has more potential and is attractive because of the nature of high efficiency and less reagent consumption, but it remains limited achievements from metallocatalytic kinetic resolution or desymmetrization by modification of the carbonyl skeleton linked to a prochiral phosphorus centre.[5] We have recently established an organocatalytic synthesis of phosphoramides with a *P*-chirogenic center as the sole chiral centre with moderate enantioselectivity,[6] demonstrating the biggest challenge in the formation of *P*-chirogenic centres: direct modification of an achiral phosphorus centre.[7] The activation of a phosphorus substrate and the interaction of the phosphorus substrate with a carbon-based chiral framework during chiral induction are not well studied.

In our research on the synthesis and application of *P*-chiral compounds, we are interested in the stereoselectivity and mechanism of the formation of *P*-chirality induced by *C*-chirality, which is believed to be on an approach to address the challenge in enantioselective synthesis of *P*-chiral phosphorus compounds. We selected *P*-chiral 1,3,2-oxazaphospholidine-2-oxides **3** containing P(V)-chiral centres as our primary subject because of their potential in catalysis and as precursors for other organophosphorus compounds.[4, 8] With this model, we have gained deep insight into the asymmetric formation of P-N and P-O bonds in the synthesis of **3** from **1** and the prolinols **2**. In previous reports of this synthesis, low to moderate diastereoselectivity was obtained without the presence of DMAP (Scheme 1).[4a-d] In this work, excellent diastereoselectivity was achieved in scalable conditions with DMAP as catalyst and the mechanism was studied. Crich has used DMAP in reactions at the P(III)-centre of *P*-chiral phosphonosugars, showing improvement of diastereoselectivity.[9] To the best of our knowledge, no such reaction on P(V)-centre has yet been described.

[a] State Key Laboratory of Polymer Physics and Chemistry, Changchun Institute of Applied Chemistry, Chinese Academy of Sciences, Changchun 130022, China. Email: kangcq@ciac.ac.cn.
[b] University of Chinese Academy of Sciences, Beijing 100049, China.
[c] Faculty of Chemistry, Northeast Normal University, Changchun 130024, China.
† Electronic Supplementary Information (ESI) available: external optimization of reaction conditions, characterization of *P*-stereogenic 1,3,2-oxazaphospholidine-2-oxides, NMR and MS analysis of the reaction mixture, computational details. See DOI: 10.1039/x0xx00000x

View Article Online
DOI: 10.1039/C6RA16686E

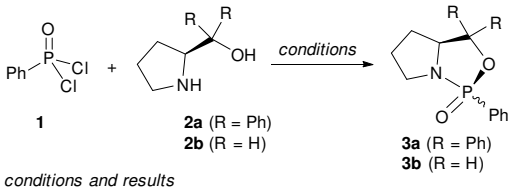

conditions and results

Reported: Et_3N, CH_2Cl_2, 0 °C, *dr* up to 87:13 for **3a**, 63:37 for **3b**

This work: DMAP, Et_3N, CH_2Cl_2, r.t., *dr* 100:0 for **3a**, 75:25 for **3b**

DMAP, imidazole, CH_2Cl_2, r.t., *dr* 91:9 for **3b**

Scheme 1 Synthesis of **3** with DMAP as organocatalyst

Results and discussion

The initial attempt for the reaction of **1** (1.5 eq) and **2a** (1.0 eq) in dichloromethane (DCM) yielded **3a** with consistent diastereoselectivity (*dr* 87:13) according to the literature,[4a] as determined by ^{1}H NMR spectroscopy (entry 1, Table 1). The reaction afforded same diastereoselectivity in chloroform and lower diastereoselectivity in toluene but did not proceed in THF or DMF (see Table S1, ESI). Surprisingly, an improvement in the diastereoselectivity to *dr* 91:9 was observed for the reaction in DCM by using DMAP (10 mol% based on **2a**) as an organocatalyst (entry 2, Table 1). The *dr* value was increased with higher DMAP loading and reached to 100:0 when a minimum of 30 mol% DMAP was used (entries 3 to 7, Table 1). Longer reaction times increased the yield (entry 8, Table 1). Gram-scale synthesis of (R_P)-**3a** under optimized conditions afforded an isolated yield of 85% from crystallization (entry 9, Table 1). We also attempted to reduce the amount of **1** used in the reaction. However, a lower dosage of **1** (1.1 eq) led to a decrease in the diastereoselectivity (Entry 10, Table 1). More experiments showed that too much DMAP did not always improve the diastereoselectivity (entries 11 to 13, Table 1). In the case of **2b** as the reaction substrate, 30 mol% DMAP improved *dr* from 63:37 to a maximum 75:25 (entries 14 to 16, Table 1). The *dr* value of the product **3b** increased to 91:9 when triethylamine was replaced with imidazole and 100 mol% DMAP was used (entry 17, Table 1). The absolute configuration of the *P*-chiral centre of **3** was confirmed by ^{1}H NMR and 2D NOESY.[4a-b]

Table 1 Conditions Optimization for Synthesis of **3**[a]

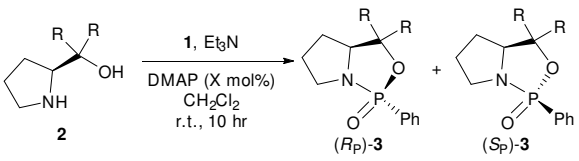

Entry	R	X	Yield[b]	*dr*[c]
1	Ph (**2a**)	0	79%	87:13
2		10	51%	91:9
3		20	56%	92:8
4		25	68%	96:4
5		30	72%	100:0
6		40	65%	100:0
7		50	78%	100:0
8[d]		30	99%	100:0
9[e]		30	85%[f]	100:0
10[g]		30	79%	79:21
11[g]		80	93%	97:3
12[g]		100	86%	93:7
13[g]		110	81%	83:17
14	H (**2b**)	0	75%	63:37
15		30	65%	75:25
16		80	75%	75:25
17[h]		50	89%	90:10

[a] Reaction conditions: **1** (0.3 mmol, 1.5 eq, otherwise indicated), **2** (0.2 mmol), triethylamine (0.6 mmol) otherwise indicated, DMAP (X mol%), CH_2Cl_2 (2 ml), r.t., 10 h otherwise indicated; [b] Of major isomer determined by ^{1}H NMR; [c] (R_P)-**3**:(S_P)-**3**, determined by ^{1}H NMR; [d] Reaction time: 24 h; [e] Starting with 2 g of **2a**; [f] Isolated yield from crystallization. [g] 0.22 mmol (1.1 eq) of **1** used. [h] Imidazole as base and see ESI for more details.

The DMAP-facilitated diastereoselectivity of the synthesis of **3** was monitored by ^{1}H NMR. Two groups of aromatic proton signals belonging to the pyridyl group of DMAP and the phenyl group of **1** were observed in a mixture of **1** and DMAP, which were assigned to DMAP trapped in *rac*-**A** and *rac*-**B** (Figure 1). The later was derived from the complexation of *rac*-**A** and another molecule of DMAP. The observations of unique A_{Ph} signals for the mixtures of DMAP and **1** at molar ratios of 1:1.5 and 0.3:1.5 suggested the presence of rapid interconversations between **1**, DMAP and *rac*-**A** (Figure S2, ESI). *rac*-**B** was the sole complex observed by ^{1}H NMR when DMAP and **1** were at a molar ratio of 2:1. The results suggested the presence of a rapid dynamic equilibrium by interconversion between both enantiomers of *P*-chiral *rac*-**A** through exchanges of chloride and DMAP at the *P*-centre.[9, 10]

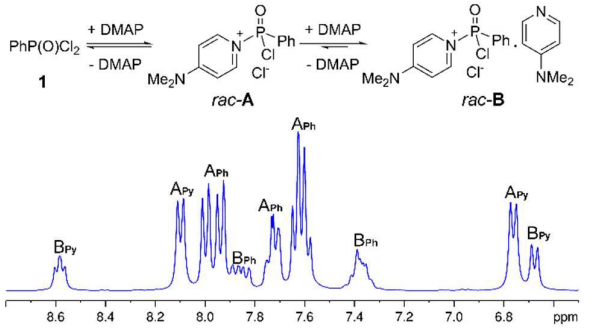

Figure 1 The interconvsions in a mixture of **1** and DMAP and corresponding ^{1}H NMR. Proton signals A_{Py} and A_{Ph} were from protons on pyridyl and phenyl trapped in balance between DMAP, **1** and *rac*-**A**. Proton signals B_{Py} and B_{Ph} were from protons on pyridyl and phenyl of *rac*-**B**.

View Article Online
DOI: 10.1039/C6RA16686E

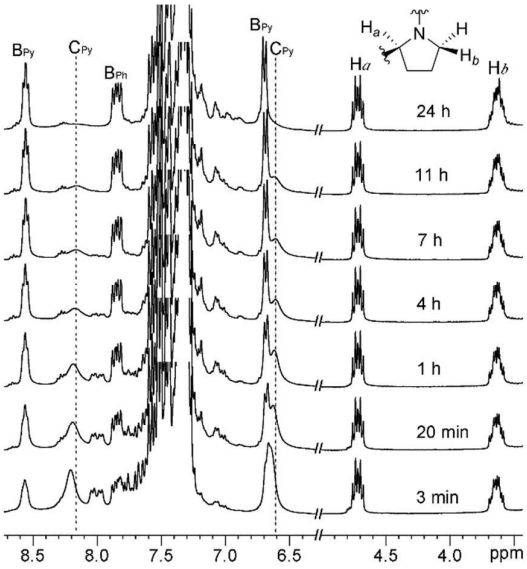

Figure 2 ^{1}H NMR trace of the reaction between **1** and **2a** in CD_2Cl_2 in the presence of DMAP. B_{Ph} and B_{Py} were the proton signals of phenyl and pyridyl of *rac*-**B**, respectively. C_{Py}s were the proton signals of pyridyl of presumed intermediate **C**, while H_a and H_b were the proton signals on pyrollidino cycle of **C** as indicated in the inset.

When **2a** was added to a mixture of **1** and DMAP in DCM, the proton signals of *rac*-**A** immediately disappeared, and no signals of **2a** were observed in the ^{1}H NMR spectra (Figure 2). A group of proton signals, C_{Py} (δ8.18 and δ6.61 ppm), assigned to the pyridyl group of a presumed intermediate **C** appeared; these signals gradually weakened and finally completely disappeared within 24 h, while the pyridyl signals (B_{Py}) of *rac*-**B** were synchronously enhanced at a level corresponding to the reduction of C_{Py}. The DMAP released from the reaction was trapped to form *rac*-**B**. DMAP in excess of **1** may result in the presence of free DMAP, which is not beneficial for improving the stereoselectivity, as shown by experiments varying the ratio of **1** and DMAP used in the reaction (entries 10 to 13, Table 1). These results suggested that *rac*-**A** was the reactive species that was converted to the presumed intermediate **C** through P-N bonding and DMAP exchange prior to the formation of the intramolecular P-O bond.

In the NMR spectra of the reaction, the signals of pyrrolidino group H_a (δ4.72 ppm) of the diastereoisomers of either **C** or **3a** overlapped; however, this was not observed for the H_b signals (δ3.63 and δ3.12 ppm, the latter was obscured by triethylamine signals). Thus, the integral ratio of $H_a/(H_a - H_b)$ was used to estimate the *dr* values of **C** and **3a**. The fact that the signals of H_a and H_b of **C** and (R_P)-**3a** maintained an integral of 1:1 suggested the presence of single diastereoisomer of both **C** and **3a** during the course of the reaction. The ^{31}P NMR monitor to the reaction showed consistent results that single diastereomer was observed during the whole reaction time (Figure S5, SI). Therefore, single stereoselectivity at the *P*-centre was determined at the stage from *rac*-**A** to **C**. One enantiomer of **C** was exclusively produced from **2a** by kinetic stereoselectivity, with a highly matched geometry of **2a** and one enantiomer of *rac*-**A**. The rapid dynamic equilibrium between enantiomers of *rac*-**A** or those of subsequent transition states result in the catalytic conversion of another enantiomer of *rac*-**A**.

In another control experiment without using triethylamine was observed the formation of (R_P)-**3a** in less than 40% yield according to ^{1}H and ^{31}P NMR track of the reaction (Figure S6 and S7, SI). An unspecified intermediate was observed and converted to (R_P)-**3a** in 88% yield on addition of triethylamine after 12 h of the reaction. Single enantiomer of unspecified intermediate and (R_P)-**3a** was observed during the whole reaction period. The results strongly supported that triethylamine was beneficial for the conversion while DMAP was a determinative factor for the diastereoselectivity.

Further insights into the high stereoselectivity induced by DMAP and the mechanism of the reaction were achieved by computer modelling using the Gaussian 09 package, in which the geometries were optimized with the B3LYP/6-31G(d, p) basis set in the solvent phase.[11] The reaction paths from both enantiomers of *rac*-**A** were considered to identify the kinetic elements of stereochemical preference in the formation of the *P*-chiral centre. From the energy profiles (Figure 3), the conversion from (S_P)-**C1** to (S_P)-**3a** crossed two higher energy barriers compared with that from (R_P)-**C1** to (R_P)-**3a**. However, these conversions should not be the determinative element for stereoselectivity because the ^{1}H NMR data did not support the presence of two epimers of **C1** or **C2**, or their interconversions.

View Article Online
DOI: 10.1039/C6RA16686E

Journal Name

ARTICLE

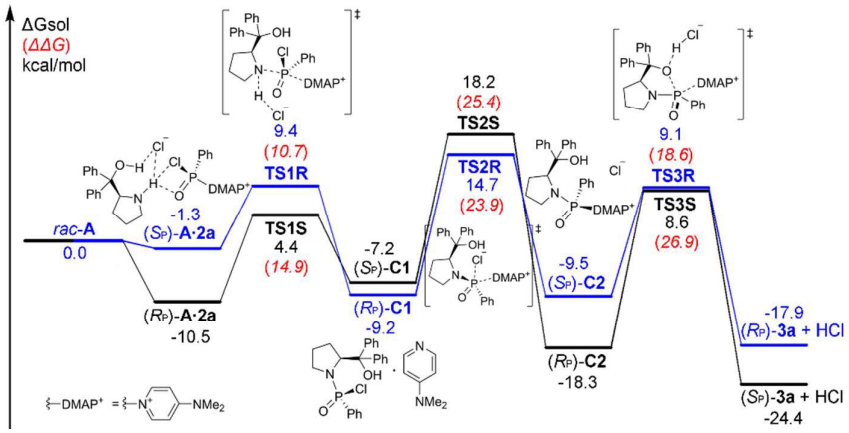

Figure 3 Free energy profile of processes from *rac*-**A** to both diastereomers of **3a**, in which were shown only the structure of the intermediates and transition states toward (R_P)-**3a**. See ESI for complete energy profile with other intermediates and transition states.

The complexes (S_P)-**A**·**2a** and (R_P)-**A**·**2a** were formed from the assembly of both (S_P)-**A** and (R_P)-**A** with **2a** through reversible intermolecular hydrogen bondings of NH(**2a**)···Cl$^-$···HO(**2a**) and PCl···NH(**2a**)···O(=P) (Figure 4). Although (R_P)-**A**·**2a** was more stable than (S_P)-**A**·**2a** according to their ΔG values in the energy profile, the formation of the P-N bond from the former to (S_P)-**C1** across the energy barrier (ΔΔG = 14.9 kcal/mol) at the transition state of **TS1S** was higher than that from the latter to (R_P)-**C1** (ΔΔG = 10.7 kcal/mol) at **TS1R** (Figure 3). Rapid consumption of (S_P)-**A**·**2a** in the formation of the P-N bond resulted in a tendency of (R_P)-**A**·**2a** to dissociate to complement the decrease of **2a**. Dissociated (R_P)-**A** would be converted to its enantiomer (S_P)-**A** through the reversible balance of *rac*-**A** with **1** or *rac*-**B**. Thus, the DMAP-catalyzed dynamic kinetic resolution of *rac*-**A** would be a key element to determine the high diastereoselectivity in the conversion from **2a** to (R_P)-**C1** (Scheme 2).[12]

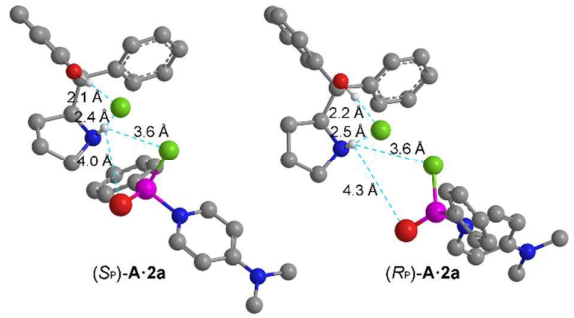

Figure 4 3D diagrams of (S_P)-**A**·**2a** and (R_P)-**A**·**2a** and hydrogen bondings in the complexes obtained from the calculations by B3LYP/6-31G(d, p).

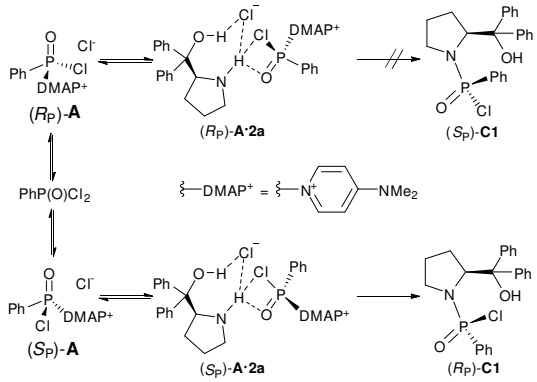

Scheme 2 Dynamic kinetic resolution of *rac*-**A**. DMAP of (S_P/R_P)-**C1** was omitted for clarity.

The intermediate (R_P)-**C1** remained in complexation with one DMAP molecule, which was converted to (S_P)-**C2** with the replacement of a chloride on phosphoryl centre by DMAP through the transition state **TS2R** with the energy barrier (ΔΔG = 23.9 kcal/mol), the highest of all the steps. The formation of the P-O bond in the conversion from (S_P)-**C2** to (R_P)-**3a** went through the transition state **TS3R** with another high-energy barrier (ΔΔG = 18.6 kcal/mol). In the favorable pathway of the (R_P)-**3a** generation, the rate-determining step was the nucleophilic addition of DMAP to the intermediate (R_P)-**C1** (**TS2R**). In the ^{1}H NMR traces of the reaction, the proton signals assigned to the presumed intermediate **C** were probably those of (R_P)-**C1**, which were indistinguishable in the NMR spectra. Electrospray ionization mass spectrometry (ESI-MS) of the

View Article Online
DOI: 10.1039/C6RA16686E

reaction mixture showed a molecular ionic peak with m/z 498.4, which supported the presence of the intermediate (R_P)-**C1** or (S_P)-**C2** (Figure S1, ESI).

Conclusions

In summary, we studied DMAP-catalyzed dynamic kinetic resolution in the prolinol-induced formation of a *P*-chirogenic centre during the synthesis of 1,3,2-oxazaphospholidine-2-oxides **3** from phenylphosphonyl dichloride **1** and prolinols **2** as a model reaction. The use of 30 mol% DMAP improved the diatereoselectivity from 87:13 to 100:0 for the synthesis of **3a** and from 63:37 to 75:25 for the synthesis of **3b**. Investigations by NMR spectra and calculations revealed the formation of an 'active phosphonyl', *rac*-**A**, from **1** and DMAP. *rac*-**A** was the key intermediate associated with **2a** prior to the P-N bond formation. The dynamic kinetic resolution of *rac*-**A** through the rapid consumption of (S_P)-**A**·**2a**, the reversible association of *rac*-**A** with **2a** and the interconversion between **1**, DMAP and *rac*-**A** determined the high diastereoselectivity in the formation of the P-N bond. The nucleophilic addition of DMAP to the intermediate (R_P)-**C1** (**TS2R**) was the rate-determining step, during which the P-N bonded intermediates **C1** were monitored by ^{1}H NMR spectra. This study revealed for the first time the mechanism of DMAP-catalyzed stereoselectivity in the formation of P-N and P-O bonds at the achiral phosphorus centre. These results would be valuable for the design of organocatalyst to induce the formation of *P*-chirogenic centres from achiral phosphorus precursors by direct asymmetric reactions at the centres.

Experimental

General information: All reagents were obtained from commercial sources and were used without further purification. The NMR spectra were recorded on Bruker Avance III with CD_2Cl_2 or $CDCl_3$ as solvent. The ^{1}H NMR were recorded at 400 MHz or 300 MHz with TMS as internal standard. The ^{13}C NMR spectra were recoded at 100 MHz with solvent as internal standard. The 31P NMR were recorded at 162 MHz with tri(o-toluyl)phosphine as internal standard. All coupling constants (*J* values) were reported in Hertz (Hz). High resolution mass spectra (HRMS) were measured using a Bruker Autoflex III MALDI-TOF mass spectrometer. The purification of products with column chromatography was performed on silica gel with 100–200 mesh.

Calculation: All calculations were performed using Gaussian 09 package. Geometries were optimized using B3LYP density functional with a basis set of 6-31G(d,p) in solvent phase considering calculation cost and pratical possibility for the size of investigated system. Solvent (DCM) effects were calculated by using the PCM solvation model. All charge distributions were calculated by Natural Bond Orbital (NBO) analysis. Computed structures are illustrated using CYLView and nonessential hydrogen atoms are omitted for clarity. All energies reported here are in Kcal/mol, and bond lengths are in angstroms (Å).

Typical procedure for the synthesis of *P*-Stereogenic 1,3,2-Oxazaphospholidine-2-oxides: DMAP (7.3 mg, 0.06 mmol, 0.3 equiv.) and a prolinol of **2a** or **2b** (0.2 mmol, 1.0 equiv.) were dissolved in DCM (2.0 mL) in ice-water bath. Triethylamine (84 uL, 0.6 mmol, 3.0 equiv.) and $PhP(O)Cl_2$ (42 uL, 0.3 mmol, 1.5 equiv) was added successively. The mixture was allowed to warm to 25 ^{o}C and stirred for 10 h. After completion of the reaction, DCM (5 mL) was added to the reaction mixture, which was washed with saturated aq. $NaHCO_3$ for three times. The organic layer were then dried over $MgSO_4$, filtered, and tri(o-toluyl)phosphine was added as internal standard. The resulting mixture was concentrated under reduced pressure. The yield and the *dr* values were determined by ^{1}H NMR.

Acknowledgements

The authors appreciate financial support by National Natural Science Foundation of China (NSFC No. 21574126).

Notes and references

1 (a) A. Grabulosa, *P-Stereogenic Ligands in Enantioselective Catalysis*; RSC Publishing: Cambridge, UK, 2011. (b) *Phosphorus Ligands in Asymmetric Catalysis. Synthesis and Applications*; A. Börner Ed.; Wiley-VCH: Weinheim, 2008.

2 For example: (a) B. Mohar, A. Čusak, B. Modec and M. Stephan, *J. Org. Chem.*, 2013, **78**, 4665; (b) A. Nakamura, T. Kageyama, H. Goto, B. P. Carrow, S. Ito and K. Nazaki, *J. Am. Chem. Soc.*, 2012, **134**, 12366; (c) A. Lapprand, M. Dutartre, N. Khiri, E. Levert, D. Fortin, Y. Rousselin, A. Soldern, S. Jugé and P. D. Harvey, *Inorg. Chem.*, 2013, **52**, 7985; (d) A. Lapprand, N. Khiri, D. Fortin, S. Jugé and P. D. Harvey, *Inorg. Chem.*, 2013, **52**, 2361; (e) H. Imoto, Y. Morisaki and Y. Chujo, *Chem. Commun.*, 2010, **46**, 7542; (f) Y. Morisaki, K. Suzuki, H. Imoto and Y. Chujo, *Macromol. Rapid Commun.*, 2010, **31**, 1719; (g) T. León, M. Parera, A. Roglans, A. Riera and X. Verdaguer, *Angew. Chem. Int. Ed.*, 2012, **51**, 6951; (h) K. Yavari, P. Retailleau, A. Voituriez and A. Marinetti, *Chem. Eur. J.*, 2013, **19**, 9939; (i) L.-I. Rodríguez, O. Rossell, M. Seco and G. Muller, *Organometallics*, 2008, **27**, 1328.

3 (a) T. Nemoto and Y. Hamada, *Tetrahedron*, 2011, **67**, 667; (b) J. S. Harvey and V. Gouverneur, *Chem. Commun.*, 2010, **46**, 7477; (c) O. I. Kolodiazhnyi, *Tetrahedron Asymmetry*, 2012, **23**, 1; (d) A. Grabulosa, J. Granell and G. Muller, *Coord. Chem. Rev.*, 2007, **251**, 25; (e) W. Tang and X. Zhang, *Chem. Rev., 20*03, **103**, 3029; (f) S. Takizawa, E. Rémond, F. A. Arteaga, Y. Yoshida, V. Sridharan, J. Bayardon, S. Jugé and H. Sasai, *Chem. Commun.*, 2013, **49**, 8392; (g) T. Imamoto, K. Tamura, Z. Zhang, Y. Horiuchi, M. Sugiya, K. Yoshida, A. Yanagisawa and I. D. Gridnev, *J. Am. Chem. Soc.*, 2012, **134**, 1754; (h) A. M. Taylor, R. A. Altman and S. L. Buchwald, *J. Am. Chem. Soc.*, 2009, **131**, 9900; (i) Z.-C. Duan, X.-P. Hu, C. Zhang and Z. Zheng, *J. Org. Chem.*, 2010, **75**, 8319; (j) R. Aznar, A. Grabulosa, A. Mannu, G. Muller, D. Sainz, V. Moreno, M. Font-Bardia, T. Calvet and J. Lorenzo, *Organometallics*, 2013, **32**, 2344; (k) X. Zhang, K. Huang, G. Hou, B. Cao and X. Zhang, *Angew. Chem. Int. Ed.*, 2010, **49**, 6421; (l) W. Tang, B. Qu, A. G. Capacci, S. Rodriguez, X. Wei, N. Haddad, B. Narayanan, S. Ma, N. Grinberg, N. K. Yee, D. Krishnamurthy, C. H. Senanayake, *Org. Lett.*, 2010, **12**, 176.

View Article Online
DOI: 10.1039/C6RA16686E

4 (a) M. P. Gamble, A. R. C. Smith and M. Wills, *J. Org. Chem.*, 1998, **63**, 6068; (b) A. Leyris, D. Nuel, L. Giordano, M. Achard, and G. Buono, *Tetrahedron Lett.*, 2005, **46**, 8677; (c) O. G. Bondarev and R. Goddard, *Tetrahedron Lett.*, 2006, **47**, 9013; (d) C. Bauduin, D. Moulin, E. B. Kaloun, C. Darcel and S. Jugé, *J. Org. Chem.*, 2003, **68**, 4293; (e) N. Khiri, E. Bertrand, M.-J. Ondel-Eymin, Y. Rousselin, J. Bayardon, P. D. Harvey, and S. Jugé, *Organometallics*, 2010, **29**, 3622; (f) G. Hoge, *J. Am. Chem. Soc.*, 2003, **125**, 10219; (g) D. Moraleda, D. Gatineau, D. Martin, L. Giordano and G. Buono, *Chem. Commun.*, 2008, 3031; (h) Q. Xu, C.-Q. Zhao and L.-B. Han, *J. Am. Chem. Soc.*, 2008, **130**, 12648; (i) D. Gatineau, L. Giordano and G. Buono, *J. Am. Chem. Soc.*, 2011, **133**, 10728.

5 (a) V. S. Chan, M. Chiu, R. G. Bergman, F. D. Toste, *J. Am. Chem. Soc.*, 2009, **131**, 6021; (b) N. F. Blank, J. R. Moncarz, T.J. Brunker, C. Scriban, B. J. Anderson, O. Amir, D. S. Glueck, L. N. Zakharov, J. A. Golen, C. D. Incarvito and A. L. Rheingold, *J. Am. Chem. Soc.*, 2007, **129**, 6847; (c) Z.-J. Du, J. Guan, G.-J. Wu, P. Xu, L.-X. Gao and F.-S. Han, *J. Am. Chem. Soc.*, 2015, **137**, 632; (d) Z.-Q. Lin, W.-Z. Wang, S.-B. Yan and W.-L. Duan, *Angew. Chem. Int. Ed.*, 2015, **54**, 6265; (e) L. Liu, A.-A. Zhang, Y. Wang, F. Zhang, Z. Zuo, W.-X. Zhao, C.-L. Feng and W. Ma, *Org. Lett.*, 2015, **17**, 2046; (f) G. Xu, M. Li, S. Wang, W. Tang, *Org. Chem. Front.*, 2015, **2**, 1342.

6 L. Wang, Z. Du, Q. Wu, R. Jin, Z. Bian, C. Kang, H. Guo, X. Ma, L. Gao, *Eur. J. Org. Chem.*, 2016, **11**, 2024.

7 (a) S. Liu, Z. Zhang, F. Xie, N. A. Butt, L. Sun and W. Zhang, *Tetrahedron Asymmetry*, 2012, **23**, 329; (b) Y. Toda, M. Pink and J. N. Johnston, *J. Am. Chem. Soc.*, 2014, **136**, 14734.

8 (a) Z. S. Han, N. Goyal, M. A. Herbage, J. D. Sieber, B. Qu, Y. Xu, Z. Li, J. T. Reeves, J.-N. Desrosiers, S. Ma, N. Grinberg, H. Lee, H. P. R. Mangunuru, Y. Zhang, D. Krishnamurthy, B. Z. Lu, J. J. Song, G. Wang and C. H. Senanayake, *J. Am. Chem. Soc.*, 2013, **135**, 2474; (b) M. P. Gamble, J. R. Studley and M. Wills, *Tetrahedron Lett.*, 1996, **37**, 2853; (c) J. M. Brown, J. V. Carey and M. J. H. Russell, *Tetrahedron*, 1990, **46**, 4877.

9 (a) A. Ferry, G. Malik, P. Retailleau, X. Guinchard and D. Crich, *J. Org. Chem.*, 2013, **78**, 6858; (b) A. Ferry, X. Guinchard, P. Retailleau and D. Crich, *J. Am. Chem. Soc.*, 2012, **134**, 12289.

10 (a) M. A. van Bochove, M. Swart and F. M. Bickelhaupt, *Phys. Chem. Chem. Phys.*, 2009, **11**, 259; (b) L. Söderberg, G. Laven, M. Kalek and J. Stawinski, *Nucleos. Nucleot. Nucl.*, 2011, **30**, 552; (c) T. León, A. Riera and X. Verdaguer, *J. Am. Chem. Soc.*, 2011, **133**, 5740; (d) V. López-Canut, J. J. Ruiz-Pernía, R. Castillo, V. Moliner and I. Tuñón, *Chem. Eur. J.*, 2012, **18**, 9612; (e) J. Beckmann and A. Schütrumpf, *Eur. J. Org. Chem.*, 2010, 363.

11 (a) A. D. Becke, *J. Chem. Phys.*, 1993, **98**, 5648; (b) A. D. Becke, *J. Chem. Phys.*, 1993, **98**, 1372.

12 (a) R. Gurubrahamam, Y. Cheng, W. Huang, K. Chen, *ChemCatChem*, 2016, **8**, 86; (b) O. Långvik, T. Saloranta, D. Y. Murzin, R. Leino, *ChemCatChem*, 2015, **7**, 4004; (c) H. Pellissier, *Adv. Synth. Cat.*, 2011, **353**, 659.

View Article Online
DOI: 10.1039/C6RA16686E

Graphic TOC

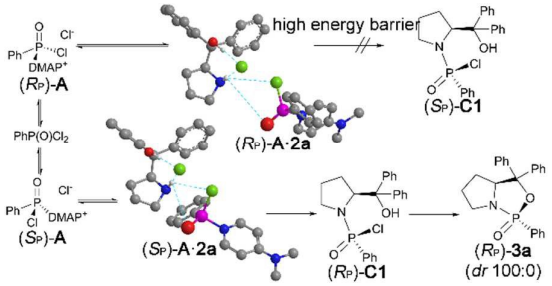

Excellent diastereoselectivity was achieved in DMAP-catalyzed P-N bonding in the synthesis of *P*-chirogenic organophosphines through dynamic kinetic resolution.